Supplementary Materials

Preparation of carbon-based metal organic frameworks modified molecularly imprinted polymers for selective recognition of bovine hemoglobin in biological samples

Xue Chen[a], Jinyue Chai[a], Baodong Sun[b], Xue Yang[a], Feng Zhang[*a], Miaomiao Tian[*a]

[*a] *Key Laboratory of Photochemical Biomaterials and Energy Storage Materials, College of Chemistry and Chemical Engineering, Harbin Normal University, Harbin, 150025, China.*

[b] *Key Laboratory for Photonic and Electronic Bandgap Materials, Ministry of Education, Harbin Normal University, Harbin, 150025, China.*

Results and discussion

Dynamic analysis

The adsorption time will affect the adsorption capacity of the adsorbent. As shown in Fig. S2, within 45 min, the adsorption capacity of C@GI@Cu-MOFs@MIPs for

* Corresponding authors *E-mail:* Zhangfeng@hrbnu.edu.cn (F. Zhang); mmttqqq@163.com (M.M. Tian).

BHb shows a trend that first increase and then stabilize. Firstly, there are many sites in the adsorbent at the initial stage of adsorption, which is conducive to the rapid combination of BHb and pores on the adsorbent surface. Secondly, after the adsorption reaches saturation, the adsorption and desorption reach an equilibrium state, so the adsorption capacity shows a stable trend. In addition, the adsorption capacity of C@GI@Cu-MOFs@MIPs is much lower than that of C@GI@Cu-MOFs@NIPs, which may be that molecular imprinting greatly increases the imprinting sites. In order to further study the adsorption mechanism of C@GI@Cu-MOFs@MIPs and C@GI@Cu-MOFs@NIPs, we analyzed their kinetic properties (Fig. S3).

In order to further investigate the adsorption properties of C@GI@Cu-MOFs@MIPs, the pseudo-first-order kinetics and pseudo-second-order kinetics adsorption processes reflected in Eq. (1) and Eq. (2) are used for the kinetics analysis of the material.

$$\ln(Q - Q_t) = \ln Q - k_1 t \quad (1)$$

$$\frac{t}{Q_t} = \frac{1}{k_2 Q^2} + \frac{t}{Q} \quad (2)$$

where Q (mg g^{-1}) and Q_t (mg g^{-1}) are adsorption capacities at equilibrium and at time t respectively, k_1 (min^{-1}) and k_2 (g mg^{-1} min^{-1}) are the adsorption rate constants of the pseudo-first-order and the pseudo-second-order dynamical process. The fitting effects of the pseudo-first-order and the pseudo-second-order dynamics models are shown in Fig. S3(A) and Fig. S3(B), respectively, and the relevant data are shown in Table S1. It

is easy to see that the adsorption of C@GI@Cu-MOFs@MIPs on BHb are more in line with the pseudo-second-order kinetic adsorption model. In addition, the initial adsorption rate h (mg g^{-1} min^{-1}) and the half equilibrium time $t_{1/2}$ (min) are also calculated by Eq. (3) and Eq. (4), respectively.

$$h = k_2 Q^2 \tag{3}$$

$$t_{1/2} = \frac{1}{k_2 Q} \tag{4}$$

where Q (mg g^{-1}) is adsorption capacities at equilibrium, and k_2 (g mg^{-1} min^{-1}) is the pseudo-second-order dynamical process.

In addition, Langmuir adsorption model and Freundlich adsorption model are further described by Eq. (5) and Eq. (6) in order to explore the binding mode of adsorbents and BHb.

$$Q = \frac{K_L Q_m C}{1 + K_L C} \tag{5}$$

$$Q = K_F C^{1/n} \tag{6}$$

where Q (mg g^{-1}) and Q_m (mg g^{-1}) are the equilibrium adsorption capacity and the maximum adsorption capacity respectively, K_L and K_F are the equilibrium adsorption constants of Langmuir and Freundlich adsorption model, C (mg L^{-1}) is the concentration at equilibrium, and n is the unitless fitting value reflects the good adsorption conditions. Fig. S3(C) and Fig. S3(D) respectively embody the fitting effects of Langmuir model

and Freundlich model, and the relevant data are shown in Table S2. The results show that the adsorption process of C@GI@Cu-MOFs@MIPs to BHb is more similar to Langmuir model, and BHb is easier to form a layer on the surface of the adsorbent.

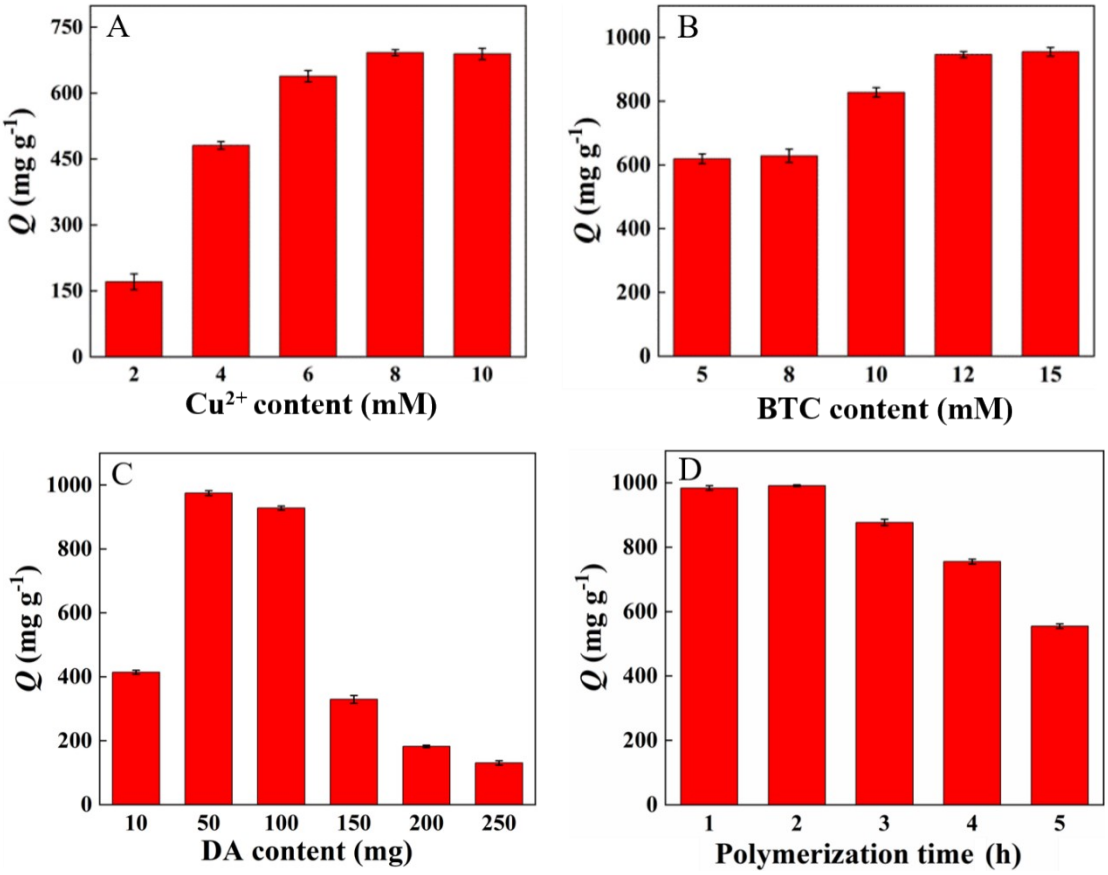

Fig. S1 Optimization of synthesis conditions. (A) Cu^{2+} content, (B) BTC content, (C) DA content, and (D) polymerization time (h).

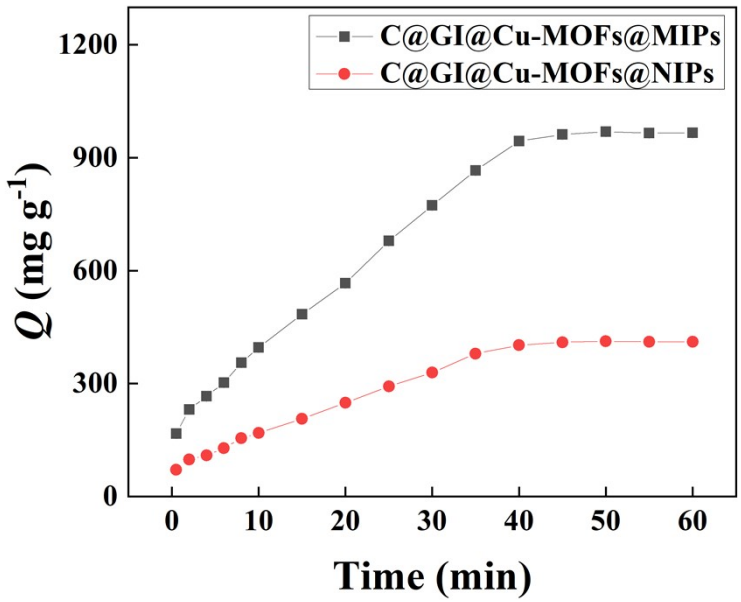

Fig. S2 Effect of adsorption time on adsorption capacity.

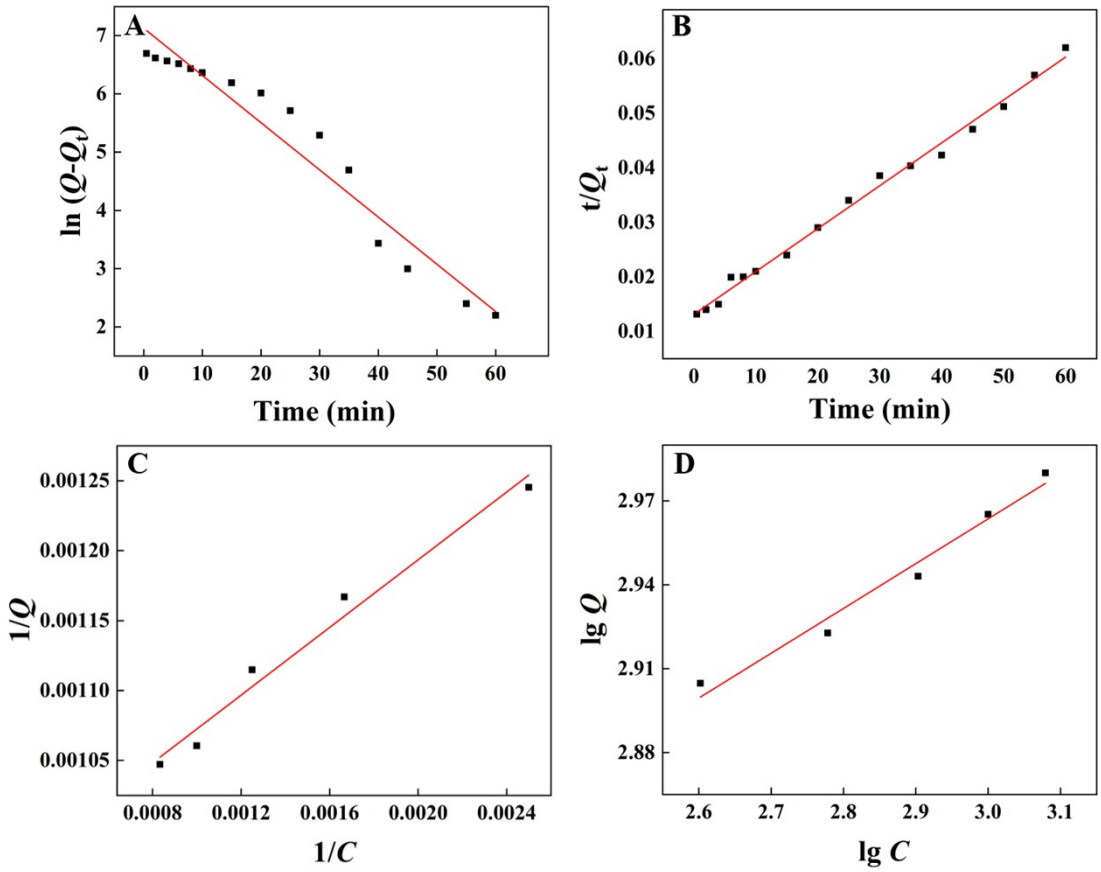

Fig. S3 (A) Pseudo-first-order kinetic model; (B) pseudo-second-order kinetic model; (C) Langmuir model; (D) Freundlich model.

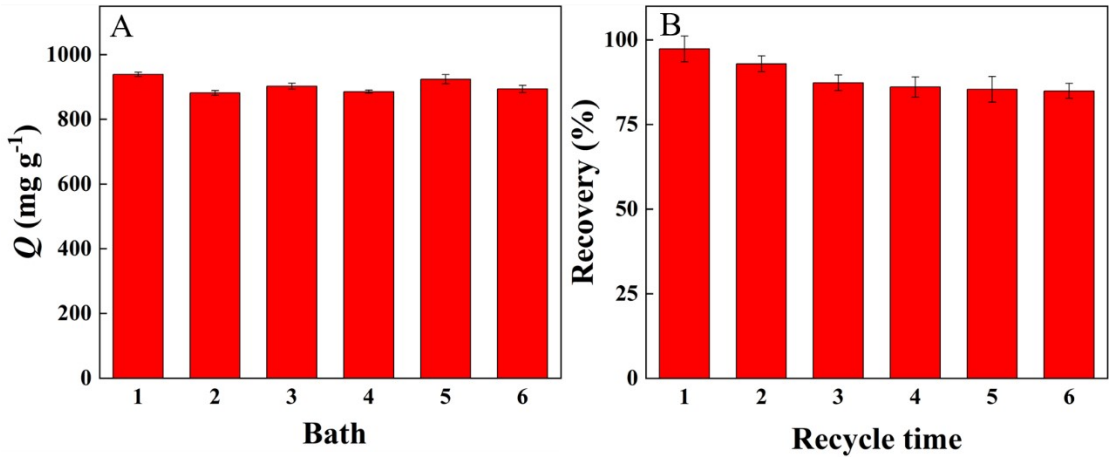

Fig. S4 Reproducibility (A) and reusability (B) of C@GI@Cu-MOFs@MIPs.

Table S1 Pseudo-first-order and pseudo-second-order adsorption kinetics model data parameters.

Adsorbets	Q_{exp} (mg g^{-1})	Pseudo-first-order kinetic model			Pseudo-second-order kinetic model			h (mg g^{-1} min^{-1})	$t_{1/2}$ (min)
		Q_{tf} (mg g^{-1})	k_1 (min^{-1})	R^2	Q_{ts} (mg g^{-1})	k_2 (g mg^{-1} min^{-1})	R^2		
C@GI@Cu-MOFs@MIPs	967.5	1245.3	8.11×10^{-2}	0.9719	1265.8	7.89×10^{-4}	0.9967	1220.5	1.02

Table S2 The data parameters of Langmuir model and Freundlich model.

Adsorbents	Langmuir model			Freundlich model		
	Q_m (mg g^{-1})	K_L (mL mg^{-1})	R^2	K_F (mg g^{-1})	$1/n$	R^2
C@GI@Cu-MOFs@MIPs	1051.1	0.0078	0.9890	300.8	0.1638	0.9836